

Correlations of spin-polarized and entangled electrons with Berry phase

Xuean Zhao^{1,2}, Hui Zhao¹, Pei Wang¹, and You-Quan Li¹

¹*Zhejiang Institute of Modern Physics, Zhejiang University, Hangzhou 310027, China*

²*National Laboratory of Solid State Microstructures, Nanjing University, Nanjing 210093, China*

The correlation and fluctuation of both entangled electrons and spin-polarized pairs affected by two rotating magnetic fields in a setup proposed by J. Carlos Egues *et al.* (Phys. Rev. Lett. **89**(2002) 176401) are studied theoretically by using scattering approach. Differing from polarized pair, the entangled electron pairs are shown to behave like a composite particle with the total spins and its z components. The singlet and triplet states exhibit different bunching and antibunching features, which can be easily adjusted by the magnetic fields. The correlations and variances can show up distinguish output signals for the four incident states. Our results are expected to be tested by using coincident technique.

PACS numbers: 72.25.-b, 72.70.+m, 03.65.Vf, 03.65.Ud

I. INTRODUCTION

Entanglement and non-locality of EPR (Einstein-Podolsky-Rosen) pairs¹ or Schrödinger cat states² are the most intriguing and profound features of quantum mechanics. They give rise to, even in the absence of interaction, correlations between spatially separated particles, which can not be described as a product of the quantum states of the two particles, and can not be explained by any local hidden variable and realistic theory.³ However, these nonclassical and non-local correlations of entanglement have been tested convincingly by Bell-inequality-type measurements in optics.^{4,5} Besides the fundamental aspects, a great deal of efforts have been made to utilize the properties of entangled particles for quantum information, quantum computation or other potential applications⁶. It is foreseeable that the realistic and applicable quantum devices should be composed of solid state elements. Therefore, it is significant and desirable to understand the entangled charged particles.

Recently, much interest has been taken in entanglement of electrons in solid state environment.^{7,8,9,10,11,12,13,14,15} Unlike photons, electrons carry charge and spin. The Coulomb interaction between electron and external electric field makes it flexible to be manipulated. Moreover, recent experiments showed that electron spin in a semiconductor has a relative long dephasing time, approximately microseconds, and it can be transported coherently over 100 micrometers¹⁶. These properties make electron a promising candidate for quantum applications. A few proposals based on electrons showed how to create an entangled pair of electrons in solid state systems, *e.g.*, superconductors^{17,18} or quantum dots^{12,13}, as a source of entangled beams of electrons.

To detect and manipulate the spin entanglement, the electric current noise of a beam splitter as a test of spin entanglement was proposed by Samuelsson *et al.*⁷, Burkard *et al.*¹³ and Carlos *et al.* In these schemes, the orbital symmetry of the entangled electron wave function can be probed directly by the current noise (shot

noise). Since the total wave function consists of orbital part and spin part, the symmetry of the orbital degree of freedom is intrinsically related to that of the spin via the Pauli exclusive principle or the parity requirement for the wave function for indistinguishable particles¹⁹. This intrinsic relation between orbital and spin in the two-electron wave function imposes an essential connection between the spin and the orbital for the entangled electrons. If one alters the spin symmetry of the pair wave function, it will definitely change the orbital symmetry of the total wave function²⁰.

Geometric phase such as Berry phase plays an important role in quantum systems with cyclic evolution. Particularly, in nanoscale electronic devices²¹, a surprising effect is that a quantum system retains a memory of its motion when it undergoes a cyclic evolution^{22,23}. In quantum information processing, Berry phase shows purely geometric characteristics that can be used to tolerate external parameter fluctuations^{24,25}. It has been shown that Berry phase can be used to implement conditional phase shifts, which gives quantum computing an ability to execute conditional dynamics between two quantum bits (qubit), where the state of one qubit affects the evolution of the other qubit during a quantum computation^{26,27}. Actually, Berry phase has been demonstrated in many systems, such as NMR^{25,28,29}, neutron beams^{30,31} and nanostructures^{32,33}, which are merely in single particle literature. Sjöqvist considered the geometric phase for entangled spin- $\frac{1}{2}$ pairs in a time-independent uniform magnetic field³⁴, and Tong *et al.* considered the geometric phase for entangled states of two spin- $\frac{1}{2}$ particles in rotating magnetic field³⁵. They showed that the geometric phase acquired by one of the entangled particles is always affected by the other particle which is even a free state. However, for unentangled particles, the geometric phase for the product state equals the sum of geometric phases acquired by each particle³⁶. Thus studies on entangled quantum systems are still in its infancy.

In this paper we study the influence of the Berry phase on the entangled states and polarized states of two spin- $1/2$ electrons by taking account of the correlation of the

two electrons. We adopt the same approach as in Ref.²⁰ and take for granted the existence of an entangler constituted by a superconductor and quantum dots^{12,17} that are in Coulomb blockade regime. The setup shown in Fig.1 consists of an entangler and a beam splitter. In this scheme, two electrons incoming from lead 1 and 2 are scattered to lead 3 and 4. Berry phase is generated by imposing an adiabatically rotating magnetic field on one of the paths of the incoming leads. The geometric phase is associated with nonvanishing dynamical phase generally. The dynamical phase ought to be diminished by some means for that it will spoil the effect of Berry phase. We use the well-developed technique, spin-echo approach^{25,37,38,39}, to compensate the dynamical phase and make the states sensitive to Berry phase.

The EPR pairs of electrons emitted from the entangler are generally singlet or triplet states^{7,12,20}. In the scheme of Ref.¹³ three triplet states can not be distinguished from each other due to the same symmetries of spatial wave functions *i.e.*, the same anti-bunching behaviors. The improved approach²⁰ can distinguish the entangled and spin polarized beams by imposing a Rashba interaction on one of the pair electrons. For the spin polarized electrons, only the polarization along z -axis is nonzero in the current autocorrelation (shot noise). The electrons polarized along y -axis show noiseless. It also shows that y component of an entangled triplet $|T_{e_y}\rangle$ and z component of unentangled triplet $|T_{u_z}\rangle$ are noisy while the triplets of entangled z component $|T_{e_z}\rangle$ and unentangled y component $|T_{u_y}\rangle$ are noiseless. We propose in this paper an approach to demonstrate the correlation of two electrons in both singlet and triplet states utilizing rotating magnetic fields. In our scheme, we employ two reversed rotating magnetic fields for one of the two electrons passing through so that their dynamic phase can be cancelled. We indicate that the correlation of the two electrons shows different values for entangled singlet state, triplet state as well as unentangled polarized states. In addition, the values of correlations can be changed by Berry phase, which gives bunching and antibunching as well as intermediate behavior as a function of rotating magnetic field parameters.

II. MODEL AND FORMULATION

The Hamiltonian of an electron in rotating magnetic fields is

$$H = H_0 - \frac{1}{2}g\mu_B\boldsymbol{\sigma} \cdot \mathbf{B}(t), \quad (1)$$

where H_0 represents a free motion and the second term represents the Zeeman energy; μ_B is the Bohr magneton, g the Landé factor and $\boldsymbol{\sigma}$ the Pauli matrices. Here $\mathbf{B}(t, x) = \mathbf{B}(t)\delta_{xx_1} - \mathbf{B}(t)\delta_{xx_2}$ are time-dependent magnetic fields located at x_1 and x_2 , respectively, and δ_{xx_i} denotes the Kronecker delta function. The orientations of the magnetic fields are opposite in direction $\vec{n}(\theta)$, as

shown in Fig.1. The rotating magnetic fields can be formed by two orthogonal magnetic fields, *i.e.*, one is along z axis with fixed magnitude while the other is rotating in x - y plane. An electron passing through such magnetic fields acquires both dynamical and geometric phases. When the magnetic field rotates slowly or adiabatically, the time evolution of the state obeys

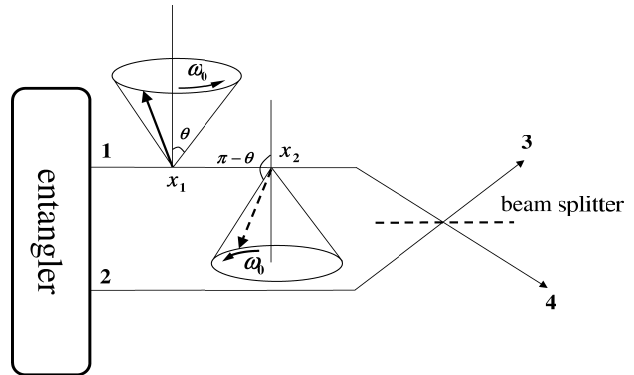


FIG. 1: A model experiment setup. The entangler emits two electrons, which are singlet or triplets. Two reversed rotating magnetic fields are located at x_1 and x_2 . The dashed line represents a beam splitter. The incoming channel 1 and channel 2 are separated in space, the exit channels are 3 and 4.

$$|\uparrow_n; t\rangle = \exp\left\{-\frac{i}{\hbar} \int E_n(\mathbf{B}(t')) dt'\right\} \exp(i\gamma_n(t)) |\uparrow_n(t)\rangle, \quad (2)$$

where n is the direction of total magnetic field in orientation $\vec{n}(\theta; t)$. $E_n = E_0 + E_{\pm}$ is an instantaneous eigenenergy in the direction of $\vec{n}(\theta; t)$. Here $E_{\pm} = \mp \frac{1}{2}g\mu_B B$ and the geometric phase is

$$\begin{aligned} \gamma_n(t) &= i \int_{\mathbf{B}(0)C}^{\mathbf{B}(t)} \langle \uparrow_n(\mathbf{B}(t')) | \nabla_{\mathbf{B}} | \uparrow_n(\mathbf{B}(t')) \rangle d\mathbf{B}(t') \\ &= i \int_{0C}^t \langle \uparrow_n(t') | \frac{\partial}{\partial t'} | \uparrow_n(t') \rangle dt', \end{aligned} \quad (3)$$

where C is the contour of a path in parameter space. The instantaneous eigenstates of the Hamiltonian (1) at time t can be expanded in the σ_z basis as

$$|\uparrow_n(t)\rangle = \cos \frac{\theta}{2} |\uparrow\rangle + \sin \frac{\theta}{2} e^{i\omega_0 t} |\downarrow\rangle \quad (4)$$

$$|\downarrow_n(t)\rangle = -\sin \frac{\theta}{2} |\uparrow\rangle + \cos \frac{\theta}{2} e^{i\omega_0 t} |\downarrow\rangle, \quad (5)$$

where $|\uparrow\rangle$ ($|\downarrow\rangle$) is eigenstate for spin up (spin down) in z axis. θ is the angle between the directions of the total magnetic field and the z axis. The level splitting in the field is

$$E_{\pm} = \mp \frac{1}{2}g\mu_B B = \mp \hbar\omega_1, \quad E_- - E_+ = 2\hbar\omega_1. \quad (6)$$

The adiabatic condition requires

$$\frac{\omega_0}{\omega_1} \ll 1, \quad (7)$$

where ω_0 is the frequency of the rotating magnetic fields and ω_1 the frequency of Rabi oscillation between the two levels. After a period $\tau = 2\pi/\omega_0$ the eigenstate $|\uparrow_n; t=0\rangle(|\downarrow_n; t=0\rangle)$ subjects to one rotating magnetic field and evolves to

$$\begin{aligned} |\uparrow_n; t=\tau\rangle &= e^{i\gamma_+(\theta)} e^{i\lambda_+} |\uparrow_n(t=0)\rangle = e^{i\gamma_+(\theta)} e^{i\lambda_+} |\uparrow_n\rangle \\ |\downarrow_n; t=\tau\rangle &= e^{i\gamma_-(\theta)} e^{i\lambda_-} |\downarrow_n(t=0)\rangle = e^{i\gamma_-(\theta)} e^{i\lambda_-} |\downarrow_n\rangle. \end{aligned} \quad (8)$$

Here γ_+ is the Berry phase picked up in the magnetic field along $\vec{n}(\theta)$, γ_- is that along $\vec{n}(\pi-\theta)$. To evaluate those Berry phases we consider the poles at the degeneracy point $\mathbf{B}=0$.

$$\nabla_{\mathbf{B}(t')} H(\mathbf{B}(t')) = -\frac{1}{2} g\mu\sigma. \quad (9)$$

$$\gamma_{\pm}(\theta) = -\frac{1}{2} \iint_{S(C)} \frac{\mathbf{B}}{B^2} \cdot d\mathbf{B} = -\frac{1}{2} \int_C d\Omega = -\frac{1}{2} \Omega(\theta) \quad (10)$$

$$\gamma_+ = -\pi(1 - \cos\theta); \text{ for } \Omega(0 \rightarrow \theta) \quad (11)$$

$$\gamma_- = -\pi(1 + \cos\theta); \text{ for } \Omega(0 \rightarrow \pi - \theta) \quad (12)$$

then one has

$$\gamma_+(\theta) = -2\pi - \gamma_-(\theta) \quad (13)$$

The global factor $\exp(iE_0t/\hbar)$ can be neglected for normalization, and λ_{\pm} 's in Eq.(8) are set to be

$$\lambda_+ = -2\pi \frac{\omega_1}{\omega_0}; \text{ and } \lambda_- = 2\pi \frac{\omega_1}{\omega_0}. \quad (14)$$

By making use of the above results we can obtain the spin states after the electron going through the two successive rotating magnetic fields or the spin-echo device

$$|\uparrow_n; t=\tau\rangle_1 = e^{i\gamma_+(\theta)} e^{i\lambda_+} |\uparrow_n\rangle_1 \quad (15)$$

$$\begin{aligned} |\downarrow_n; t=\tau\rangle_2 &= e^{i\gamma_-(\pi-\theta)} e^{i\lambda_-} |\downarrow_n; t=0\rangle_2 \\ &= e^{i\gamma_-(\pi-\theta)} e^{i\lambda_-} |\uparrow_n; t=\tau\rangle_1 \\ &= e^{i\gamma_+(\theta)} e^{i\lambda_-} e^{i\gamma_+(\theta)} e^{i\lambda_+} |\uparrow_n; t=0\rangle_1 \\ &= e^{2i\gamma_+(\theta)} |\uparrow_n\rangle_1. \end{aligned} \quad (16)$$

Here the suffix 1 or 2 refers the first or second magnetic field. Similarly, one has

$$|\downarrow_n; t=\tau\rangle_1 = e^{i\gamma_-(\theta)} e^{i\lambda_-} |\downarrow_n; t=0\rangle_1 \quad (17)$$

$$\begin{aligned} |\uparrow_n; t=\tau\rangle_2 &= e^{i\gamma_+(\pi-\theta)} e^{i\lambda_+} |\uparrow_n; t=0\rangle_2 \\ &= e^{i\gamma_+(\pi-\theta)} e^{i\lambda_+} |\downarrow_n; t=\tau\rangle_1 \\ &= e^{i\gamma_-(\theta)} e^{i\lambda_+} e^{i\gamma_-(\theta)} e^{i\lambda_-} |\downarrow_n; t=0\rangle_1 \\ &= e^{2i\gamma_-(\theta)} |\downarrow_n\rangle_1 \end{aligned} \quad (18)$$

Consequently, an electron passing through the aforementioned two successive rotating magnetic fields evolves to

$$\begin{aligned} |\uparrow_n\rangle &\xrightarrow{2\tau} e^{2i\gamma_+(\theta)} |\uparrow_n\rangle \\ |\downarrow_n\rangle &\xrightarrow{2\tau} e^{2i\gamma_-(\theta)} |\downarrow_n\rangle \end{aligned} \quad (19)$$

Which can be written in a matrix form

$$\begin{pmatrix} a_{1\uparrow_n}^+(2\tau) \\ a_{1\downarrow_n}^+(2\tau) \end{pmatrix} = \begin{pmatrix} e^{2i\gamma_+(\theta)} & 0 \\ 0 & e^{2i\gamma_-(\theta)} \end{pmatrix} \begin{pmatrix} a_{1\uparrow_n}^+(0) \\ a_{1\downarrow_n}^+(0) \end{pmatrix} \quad (20)$$

where $a_{1\uparrow_n}^+(2\tau)$ and $a_{1\downarrow_n}^+(2\tau)$ create electrons with spin in direction of $\vec{n}(\theta, 2\tau)$ and $\vec{n}(\pi-\theta, 2\tau)$, respectively, in channel 1 after a period 2τ . This gives the spin states $|\uparrow_n(t)\rangle$ and $|\downarrow_n(t)\rangle$ at the beam splitter after interacting with two successive opposite rotating magnetic fields in channel 1. In terms of the inverse relation of Eq.(4) and (5), one can transform Eq.(20) into the σ_z representation,

$$\begin{pmatrix} a_{1\uparrow}^+ \\ a_{1\downarrow}^+ \end{pmatrix} = \begin{pmatrix} e^{-2i\gamma_+(\theta)} \cos \frac{\theta}{2} & -e^{-2i\gamma_-(\theta)} \sin \frac{\theta}{2} \\ e^{-2i\gamma_+(\theta)} \sin \frac{\theta}{2} & e^{-2i\gamma_-(\theta)} \cos \frac{\theta}{2} \end{pmatrix} \begin{pmatrix} a_{1\uparrow_n}^+(2\tau) \\ a_{1\downarrow_n}^+(2\tau) \end{pmatrix}, \quad (21)$$

where $a_{1\uparrow}^+$ and $a_{1\downarrow}^+$ create electrons in the direction of z and $-z$, respectively, in channel 1 after a period 2τ . The spin states in channel 2 undergo a free motion before passing through the beam splitter. It can be written as

$$\begin{pmatrix} a_{2\uparrow}^+ \\ a_{2\downarrow}^+ \end{pmatrix} = \begin{pmatrix} \cos \frac{\theta}{2} & -\sin \frac{\theta}{2} \\ \sin \frac{\theta}{2} & \cos \frac{\theta}{2} \end{pmatrix} \begin{pmatrix} a_{2\uparrow}^+(2\tau) \\ a_{2\downarrow}^+(2\tau) \end{pmatrix}. \quad (22)$$

At the beam splitter the electrons are scattered into outgoing channels 3 and 4. The output can be expressed in terms of scattering matrix of the beam splitter

$$\begin{pmatrix} a_{3\uparrow}^+ \\ a_{3\downarrow}^+ \\ a_{4\uparrow}^+ \\ a_{4\downarrow}^+ \end{pmatrix} = \begin{pmatrix} r & 0 & t & 0 \\ 0 & r & 0 & t \\ t & 0 & r & 0 \\ 0 & t & 0 & r \end{pmatrix} \begin{pmatrix} a_{1\uparrow}^+(2\tau) \\ a_{1\downarrow}^+(2\tau) \\ a_{2\uparrow}^+(2\tau) \\ a_{2\downarrow}^+(2\tau) \end{pmatrix}, \quad (23)$$

where $a_{3\uparrow}^+$ and $a_{3\downarrow}^+$ create electrons with spin in direction of $\vec{n}(\theta, 2\tau)$ and $\vec{n}(\pi-\theta, 2\tau)$, respectively, in channel 3. It is the same for $a_{4\uparrow}^+$ and $a_{4\downarrow}^+$ in channel 4. The combination of these two processes gives rise to

$$\begin{pmatrix} a_{3\uparrow}^+ \\ a_{3\downarrow}^+ \\ a_{4\uparrow}^+ \\ a_{4\downarrow}^+ \end{pmatrix} = \begin{pmatrix} r(\cos 2\gamma_- - i \cos \theta \sin 2\gamma_-) & -ir \sin \theta \sin(2\gamma_-) & t & 0 \\ -ir \sin \theta \sin(2\gamma_-) & r(\cos 2\gamma_- + i \cos \theta \sin 2\gamma_-) & 0 & t \\ t(\cos 2\gamma_- - i \cos \theta \sin 2\gamma_-) & -it \sin \theta \sin(2\gamma_-) & r & 0 \\ -it \sin \theta \sin(2\gamma_-) & t(\cos 2\gamma_- + i \cos \theta \sin 2\gamma_-) & 0 & r \end{pmatrix} \begin{pmatrix} a_{1\uparrow}^+ \\ a_{1\downarrow}^+ \\ a_{2\uparrow}^+ \\ a_{2\downarrow}^+ \end{pmatrix}, \quad (24)$$

where $a_{3\uparrow}^+$ and $a_{3\downarrow}^+$ create electrons in the direction of z and $-z$, respectively, in outgoing channel 3 after a period 2τ . The notation implications for $a_{4\uparrow}^+$ and $a_{4\downarrow}^+$ are similar. In scattering matrix language it is

$$\begin{pmatrix} a_{3\uparrow} \\ a_{3\downarrow} \\ a_{4\uparrow} \\ a_{4\downarrow} \end{pmatrix} = \begin{pmatrix} s_{3\uparrow,1\uparrow} & s_{3\uparrow,1\downarrow} & s_{3\uparrow,2\uparrow} & s_{3\uparrow,2\downarrow} \\ s_{3\downarrow,1\uparrow} & s_{3\downarrow,1\downarrow} & s_{3\downarrow,2\uparrow} & s_{3\downarrow,2\downarrow} \\ s_{4\uparrow,1\uparrow} & s_{4\uparrow,1\downarrow} & s_{4\uparrow,2\uparrow} & s_{4\uparrow,2\downarrow} \\ s_{4\downarrow,1\uparrow} & s_{4\downarrow,1\downarrow} & s_{4\downarrow,2\uparrow} & s_{4\downarrow,2\downarrow} \end{pmatrix} \begin{pmatrix} a_{1\uparrow} \\ a_{1\downarrow} \\ a_{2\uparrow} \\ a_{2\downarrow} \end{pmatrix}, \quad (25)$$

where the s-matrix satisfies

$$S^\dagger S = S S^\dagger = I \quad (26)$$

and then the Eq.(25) can be written in a more compact form

$$a_{k\sigma} = \sum_{l\sigma'} s_{k\sigma,l\sigma'} a_{l\sigma'}; \quad k \in 3, 4; \quad l \in 1, 2; \quad \sigma, \sigma' \in \uparrow, \downarrow. \quad (27)$$

The creation and annihilation operators obey the conventional communication relations

$$[a_{l\sigma}, a_{l'\sigma'}^\dagger] = \delta_{ll'} \delta_{\sigma\sigma'} \quad l, l' \in 1, 2; \quad \sigma, \sigma' \in \uparrow, \downarrow \quad (28)$$

and the outgoing operators also obey the communication relations

$$[a_{k\sigma}, a_{k'\sigma'}^\dagger] = \delta_{kk'} \delta_{\sigma\sigma'} \quad k, k' \in 3, 4; \quad \sigma, \sigma' \in \uparrow, \downarrow. \quad (29)$$

The incident operators $a_{l\sigma}$ and outgoing operators $a_{k\sigma'}^\dagger$ satisfy the following relations

$$[a_{l\sigma}, a_{k\sigma'}^\dagger] = s_{k\sigma',l\sigma}^* \quad l \in 1, 2; \quad k \in 3, 4 \quad (30)$$

With relations Eqs.(26-30), we are in the position to calculate physical observable. In this paper we are interested in the correlations of two electrons forming entangled states or polarized states. There are four kind of states emitted from the entangler. One is singlet with total spin zero and the others are three triplets with total spin one. The scattering region involves interaction with magnetic fields and the beam splitter. The incident singlet state is denoted by $|\Psi_S\rangle = 1/\sqrt{2}(a_{1\uparrow}^+ a_{2\downarrow}^+ - a_{1\downarrow}^+ a_{2\uparrow}^+) |0\rangle$ and the entangled triplet state is denoted by $|\Psi_{T_e}\rangle = 1/\sqrt{2}(a_{1\uparrow}^+ a_{2\downarrow}^+ + a_{1\downarrow}^+ a_{2\uparrow}^+) |0\rangle$. The other two unentangled triplet states are $|\Psi_{T_u}\rangle = a_{1\uparrow}^+ a_{2\uparrow}^+ |0\rangle$ and $|\Psi_{T_d}\rangle = a_{1\downarrow}^+ a_{2\downarrow}^+ |0\rangle$ for spins in parallel upward and downward in z axis respectively. The suffix 1 refers for channel 1 and the suffix 2 for channel 2 as shown in Fig. 1. The two electrons emitted from the entangler are spatially separated in each channel due to the Coulomb blockade occurring in the quantum dots^{7,17}. The electron in channel 1 is scattered by the rotating magnetic fields picking up a geometric phase and then moves to the beam splitter. The two electrons interact at the beam splitter and move to the output channel 3 or 4. The outgoing amplitudes of electron waves in probe 3 and 4 are determined by Eq.(24), i.e., $|\text{out}\rangle = S^\dagger |\text{in}\rangle$. In terms of S-matrix the incoming states are related to the outgoing states by $|\text{in}\rangle = S |\text{out}\rangle$ due to the unitary condition of s-matrix given in Eq.(26).

The incoming states can be conveniently expressed by outgoing states in operator form

$$\begin{cases} |\Psi_S\rangle \\ |\Psi_{T_e}\rangle \end{cases} = \frac{1}{\sqrt{2}}(a_{1\uparrow}^+ a_{2\downarrow}^+ \mp a_{1\downarrow}^+ a_{2\uparrow}^+) |0\rangle \\ = \frac{1}{\sqrt{2}} \left[\left\{ \frac{P}{\tilde{P}} (a_{3\uparrow}^+ a_{3\downarrow}^+ + a_{4\uparrow}^+ a_{4\downarrow}^+) + \left\{ \frac{Q}{\tilde{Q}} a_{3\uparrow}^+ a_{4\downarrow}^+ + \left\{ \frac{M}{\tilde{M}} a_{3\downarrow}^+ a_{4\uparrow}^+ + \left\{ \frac{D}{\tilde{D}} (a_{3\uparrow}^+ a_{4\uparrow}^+ + a_{3\downarrow}^+ a_{4\downarrow}^+) \right\} \right\} \right\} \right] |0\rangle \quad (31)$$

$$|\Psi_u\rangle = a_{1\uparrow}^+ a_{2\uparrow}^+ |0\rangle = \left[P_u a_{3\uparrow}^+ a_{4\uparrow}^+ + Q_u (a_{3\downarrow}^+ a_{3\uparrow}^+ + a_{4\downarrow}^+ a_{4\uparrow}^+) + S_u (r^{*2} a_{3\downarrow}^+ a_{4\uparrow}^+ - t^{*2} a_{3\uparrow}^+ a_{4\downarrow}^+) \right] |0\rangle \quad (32)$$

$$|\Psi_d\rangle = a_{1\downarrow}^+ a_{2\downarrow}^+ |0\rangle = \left[P_d a_{3\downarrow}^+ a_{4\downarrow}^+ + Q_d (a_{3\uparrow}^+ a_{3\downarrow}^+ + a_{4\uparrow}^+ a_{4\downarrow}^+) + S_d (r^{*2} a_{3\uparrow}^+ a_{4\downarrow}^+ - t^{*2} a_{3\downarrow}^+ a_{4\uparrow}^+) \right] |0\rangle \quad (33)$$

where

$$P = 2r^* t^* \cos 2\gamma_-; \quad \tilde{P} = 2ir^* t^* \cos \theta \sin 2\gamma_-$$

$$Q = (r^{*2} + t^{*2}) \cos 2\gamma_- + i(r^{*2} - t^{*2}) \cos \theta \sin 2\gamma_-$$

$$\begin{aligned}
\tilde{Q} &= (r^{*2} - t^{*2}) \cos 2\gamma_- + i(r^{*2} + t^{*2}) \cos \theta \sin 2\gamma_- \\
M &= -[(r^{*2} + t^{*2}) \cos 2\gamma_- + i(t^{*2} - r^{*2}) \cos \theta \sin 2\gamma_-] \\
\tilde{M} &= (r^{*2} - t^{*2}) \cos 2\gamma_- - i(r^{*2} + t^{*2}) \cos \theta \sin 2\gamma_- \\
D &= i \sin \theta \sin 2\gamma_- (r^{*2} - t^{*2}) \\
\tilde{D} &= i \sin \theta \sin 2\gamma_- (r^{*2} + t^{*2}) \\
P_u &= (\cos 2\gamma_- + i \sin 2\gamma_- \cos \theta)(r^{*2} - t^{*2}) \\
P_d &= (\cos 2\gamma_- - i \sin 2\gamma_- \cos \theta)(r^{*2} - t^{*2}) \\
Q_u &= ir^*t^* \sin \theta \sin(2\gamma_-) \\
Q_d &= ir^*t^* \sin \theta \sin(2\gamma_-) \\
S_u &= i \sin \theta \sin(2\gamma_-) \\
S_d &= i \sin \theta \sin(2\gamma_-).
\end{aligned}$$

The probabilities of the electron with spin σ appearing at output probes 3 and 4 can be evaluated by

$$\langle \Psi_j | n_{l\sigma} | \Psi_j \rangle \quad \text{or} \quad \langle \Psi_j | n_{l\sigma} n_{l'\sigma'} | \Psi_j \rangle, \quad (34)$$

where j is label for the singlet and triplets, and $l, l' \in 3, 4$, $\sigma, \sigma' \in \uparrow, \downarrow$. For instance, $j = T_e$ and $l = 3, l' = 4$. $\sigma = \uparrow$ and $\sigma' = \downarrow$. One has to evaluate the expectation that one electron appears at the output probe 3 with spin up and the other electron appears at the output probe 4 with spin down simultaneously for the incident state $|\Psi_{T_e}\rangle$.

$$\begin{aligned}
&\langle \Psi_{T_e} | n_{3\uparrow} n_{4\downarrow} (1 - n_{3\downarrow})(1 - n_{4\uparrow}) | \Psi_{T_e} \rangle \\
&= \langle \Psi_{T_e} | a_{3\uparrow}^+ a_{3\uparrow} a_{4\downarrow}^+ a_{4\downarrow} (1 - a_{3\downarrow}^+ a_{3\downarrow})(1 - a_{4\uparrow}^+ a_{4\uparrow}) | \Psi_{T_e} \rangle \\
&= \langle \Psi_{T_e} | a_{3\uparrow}^+ a_{4\downarrow}^+ a_{4\downarrow} a_{3\uparrow} | \Psi_{T_e} \rangle \\
&= \sum_m \langle \Psi_{T_e} | a_{3\uparrow}^+ a_{4\downarrow}^+ | m \rangle \langle m | a_{4\downarrow} a_{3\uparrow} | \Psi_{T_e} \rangle \\
&= \sum_m |\langle m | a_{4\downarrow} a_{3\uparrow} | \Psi_{T_e} \rangle|^2 \\
&= \frac{1}{2} \sum_m |\langle m | a_{4\downarrow} a_{3\uparrow} (a_{1\uparrow}^+ a_{2\downarrow}^+ - a_{1\downarrow}^+ a_{2\uparrow}^+) | 0 \rangle|^2,
\end{aligned}$$

where m runs over all the states that constitute a complete set of Hilbert space. We have dropped terms involving more than three annihilation operators, such as $a_{3\uparrow} a_{3\downarrow} a_{4\downarrow}$ due to the Pauli exclusive principle. Using Eqs.(31)-(33) and commutation relations of output operators $a_{3\sigma}^+$ and $a_{4\sigma}^+$, one can obtain the output mean electron numbers, variances and correlations for the input states, *i.e.*, the singlet and triplet states. The results are summarized in the TABLE I and TABLE II. The TABLE III is the input mean numbers, variance and correlations for the four incident states.

III. RESULTS AND DISCUSSIONS

TABLE I gives the output correlations and average numbers of electrons and TABLE II gives output variances of electrons for input singlet and triplet states. As a comparison we list input correlations, average occupations and variances of electrons for input singlet and triplet states in TABLE III. Our discussions contain the following parts

A. The average occupation in one output channel

Firstly one can see that in the output channels the average numbers of electrons are constant values 0.5 for the entangled singlet states whether the entangled singlet state is scattered or not (see TABLE I and TABLE III rows 2 to 5 and column 2). They are irrelevant to magnetic field and the beam splitter. However, for the incident entangled triplet state the output average numbers of electrons are dependent on Berry phase (see TABLE I rows 2 to 5 and column 3). In comparison to the initial average numbers of electrons (see TABLE III rows 2 to 5 and column 3), the scattered entangled triplet state acquires additional phase. These results indicate that the singlet state does not acquire a phase in the rotating magnetic fields. It is just like a composite particle with zero spin, as shown by Fig. 2a. In Fig. 2a the two spins are always aligned opposite direction. They form a composite particle with the total spin zero $S_T = 0$. In this case the z components of the two electrons are opposite in direction and the composite particle is just the singlet. With this notation in mind the entangled triplet state should acquire Berry phase due to its total spin $S_T = 1$, although the total projection of spin along z direction is zero, (see TABLE I rows 2 to 5 and column 3 and Fig. 2b). The average output numbers of electrons are related to Berry phase for the input polarized triplet states. But they are different from that of the entangled triplet state. For example, in the input polar-

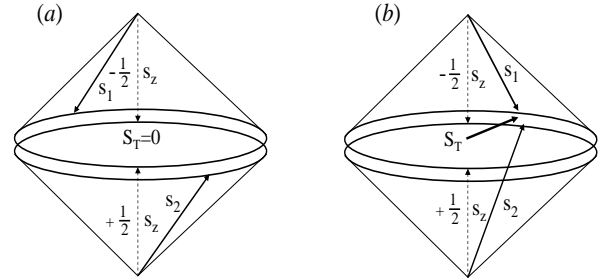


FIG. 2: The composition of two electron spins. (a) the singlet state composed of two opposite spins s_1 and s_2 and their z components. The total spin S_T and the total z component are zero. (b) The triplet with its zero z component. The two spins s_1 and s_2 are not opposite and form a total spin $S_T = 1$.

ized state $|\Psi_{T_u}\rangle = a_{1\uparrow}^+ a_{2\uparrow}^+ |0\rangle = |\uparrow\rangle_1 \otimes |\uparrow\rangle_2$ the electron in channel 1 with spin-up subjects the rotating magnetic fields and is scattered at the beam splitter. The reduced part of $\langle \Psi_{T_u} | n_{3\uparrow} | \Psi_{T_u} \rangle$ is $R\Theta$. This is just the reflected spin flipped part of spin-up in channel 1 into spin-down. Viewing $\langle \Psi_{T_u} | n_{3\downarrow} | \Psi_{T_u} \rangle = R\Theta$ one finds that the contri-

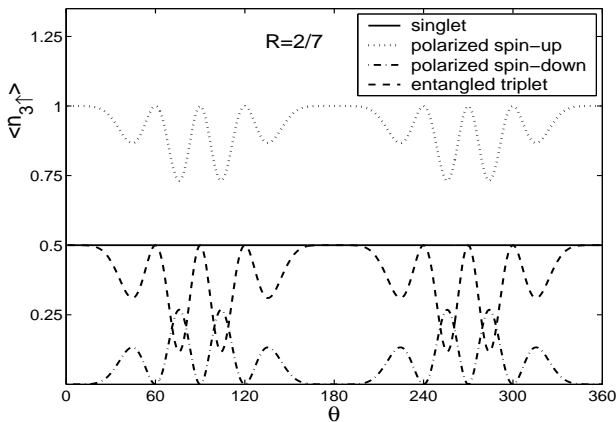


FIG. 3: The average occupation probabilities of the spin-up in the output channel 3 for different incident states. The constant value 0.5 is for the incident singlet state and shown by the solid line. The dashed line is for the incident entangled triplet state. The dotted line is for the incident spin-up polarized state and the dash-dotted line is for the incident spin-down polarized state. The beam-splitter is asymmetric with the reflection probability $R = 2/7$.

bution of the spin flipped part is precisely $R\Theta$. Similar analysis shows that the spin flipped part is $T\Theta$ for channel 1 electrons, which transmit to the output channel 4. It can also be seen clearly by setting the total reflection beam splitter, i.e., $R = 1$. In this condition the electron in channel 1 directly goes to the output channel 3 and the electron in channel 2 directly goes to the output channel 4. Because the rotating magnetic fields are located in the channel 1, the transmission of an electron from the channel 2 to the channel 4 is unit for the spin conserved processes (i.e., the spin-up to spin-up and spin-down to spin-down) and zero for spin flipped processes (i.e., spin-up to spin-down and spin-down to spin-up). It is verified in TABLE I rows 4 and 5, columns 4 and 5 by setting $T = 0$. Fig. 3 and Fig. 4 show the variations of the occupation probability and its mean square fluctuation of the spin-up electrons in the output channel 3 with the angle θ , which is the polar angle of the total magnetic field along z -axis, as shown in Fig. 1. The beam splitter is asymmetric by taking reflection coefficient $R = 2/7$. From Fig. 3 and Fig. 4 one can see that the averages $\langle n_{3\uparrow} \rangle$ are different functions of θ for each incident state, which can be controlled by B_z due to $\tan\theta = B_{\perp}/B_z$. B_{\perp} is a rotating magnetic field in x - y plane whose magnitude is fixed. B_z is a constant magnetic field along z axis which can be controlled by the external means. From above results and discussions it can motivate us to use a counter detector to distinguish the four states by varying the magnetic field B_z .

B. The same output channel with different spins

From rows 6 to 7 in TABLE I and TABLE II, one can see that the correlations $\langle n_{3\uparrow}n_{3\downarrow} \rangle$ and $\langle n_{4\uparrow}n_{4\downarrow} \rangle$ are dif-

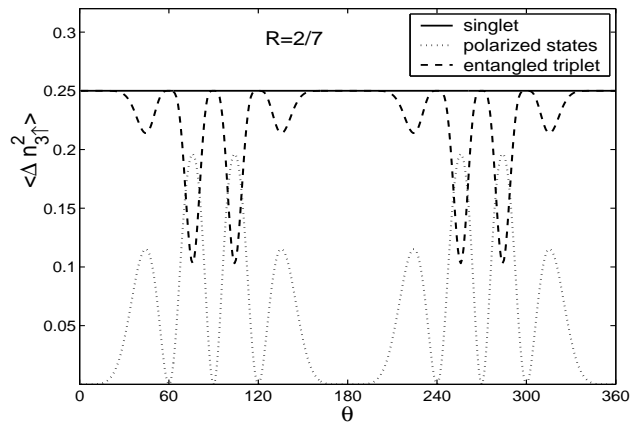


FIG. 4: The variances of the spin-up in the output channel 3 for different incident states. The constant value 0.25 is for the incident singlet state and shown by the solid line. The dashed line is for the incident entangled triplet state. The dotted line is for both the incident spin-up and spin-down polarized states. The beam-splitter is the same as that in Fig. 3.

ferent for entangled singlet and triplet states, whereas the same for unentangled states. In the entangled singlet state the correlation of $\langle \Psi_S | n_{3\uparrow}n_{3\downarrow} | \Psi_S \rangle$ reaches the maximum $2RT$ and minimum 0, by viewing a cosine function in the expression $\langle \Psi_S | n_{3\uparrow}n_{3\downarrow} | \Psi_S \rangle = 2RT \cos^2 2\gamma_{-}$. The correlations oscillate with respect to the angle θ , as shown by solid line in Fig. 5. In Fig. 5 the dashed line represents the correlation for the input entangled triplet. One can see that it oscillates but the amplitude is less than that of the singlet. The dotted line is for two polarized states. Fig. 6 shows the variances $\langle \Delta n_{3\uparrow} \Delta n_{3\downarrow} \rangle$ for incident states. It shows that the variance of the input singlet state oscillates positively and negatively.

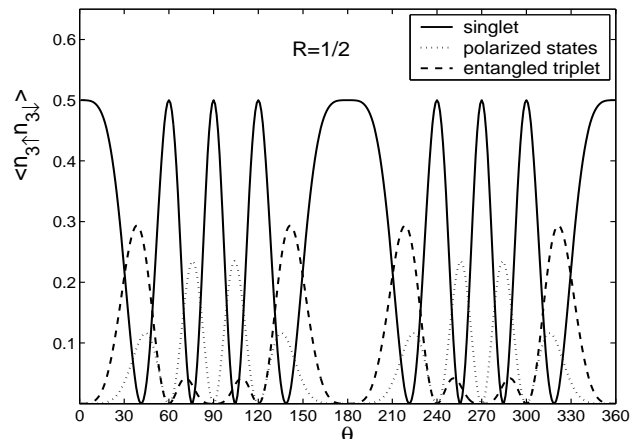


FIG. 5: The correlations of the spin-up and spin-down in the same output channel 3 for different incident states. The solid line is for the singlet state. The dashed line is for the incident entangled triplet state. The dotted line is for both the incident spin-up and spin-down polarized states. The beam-splitter is an ideal device with the ratio of reflection to transmission 50:50.

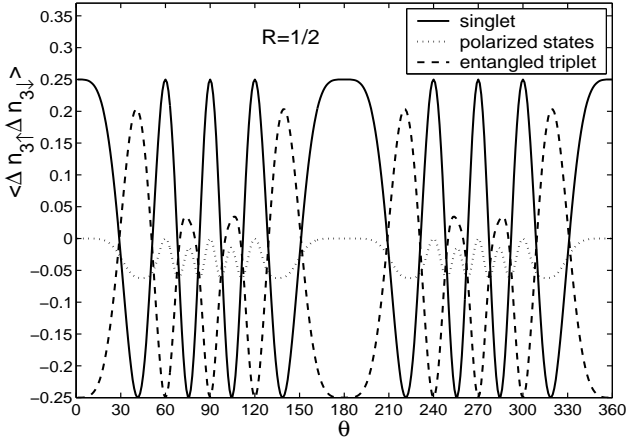


FIG. 6: The variances of the spin-up and spin-down in the same output channel 3 for different incident states. The solid line is for the entangled singlet state. The dashed line is for the incident entangled triplet state. The dotted line is for both the incident spin-up and spin-down polarized states. The beam-splitter is the same as Fig. 5.

When the variance is positive the two electrons prefer to reach the same output channel, bunching behavior. When the variance is negative, they prefer to separate to different output channels, antibunching behavior. Due to Berry phase picked up by spins passing through the rotating magnetic fields, the symmetry of the wave function is changed. The correlation $\langle n_{3\uparrow} n_{3\downarrow} \rangle$ goes to zero at $\theta = 41.4^\circ, 75.5^\circ, 104.5^\circ$ and 138.6° , and reaches the maximum at $\theta = 0^\circ, 60^\circ, 90^\circ, 120^\circ$ and 180° for the singlet state and an ideal beam splitter, $R = T = 1/2$. Correspondingly, the variances $\langle \Delta n_{3\uparrow} \Delta n_{3\downarrow} \rangle$ reach maximal positive and negative values at these angles for the singlet state. For the entangled triplet the situation is reversed. At $\theta = 41.4^\circ, 75.5^\circ, 104.5^\circ$ and 138.6° the correlations are maximum and at $\theta = 0^\circ, 60^\circ, 90^\circ, 120^\circ$ and 180° are minimum. The variances $\langle \Delta n_{3\uparrow} \Delta n_{3\downarrow} \rangle$ are always negative showing the antibunching property for the polarized states, as shown by dotted line in Fig. 6. The same analysis is applied for the output channel 4.

C. The output correlations of different channels with the same spins

The correlations $\langle n_{3\uparrow} n_{4\uparrow} \rangle$ and $\langle n_{3\downarrow} n_{4\downarrow} \rangle$ are different for the entangled singlet and triplet states. They also differ from that of unentangled triplet states $|\Psi_{T_u}\rangle$ and $|\Psi_{T_d}\rangle$. From TABLE I and TABLE II rows 8 to 9 one can find that the correlation is definite 0 for the input state $|\Psi_{T_d}\rangle$. This is due to the particle property of an electron. The particle occurs only at one position at a time, although there is a probability to flip a spin in channel 1 for the incident spin-down state $|\Psi_{T_d}\rangle = a_{1\downarrow}^+ a_{2\downarrow}^+ |0\rangle$ splitting into the output channel 3 and 4. The particle cannot be partially reflected to channel 3 and partially

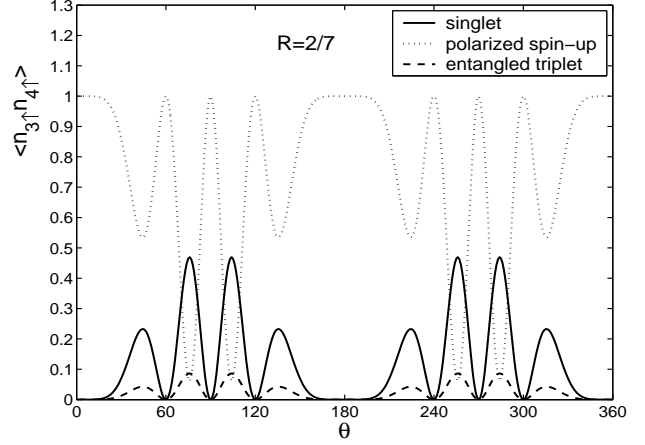


FIG. 7: The correlations of spin-up and spin-up in different output channels 3 and 4 for the unsymmetrical beam splitter. The reflection of the beam splitter is $R = 2/7$. The solid line is for singlet and the dashed line is for the entangled triplet. The dotted line is for spin-up polarized state. The correlation of the spin-down polarized state is constant zero.

transmitted to channel 4 simultaneously. If the magnetic fields is removed, the correlations become 0 for the entangled states and 1 for the spin-up polarized state. Under this condition the variance $\langle \Delta n_{3\uparrow} \Delta n_{4\uparrow} \rangle$ is 0 for unentangled states and $-1/4$ for the entangled states. These results manifest that the electrons with spin-up in channel 3 and 4 cannot appear simultaneously in the input state $|\Psi_{T_d}\rangle$. In addition the fluctuation $\langle \Delta n_{3\uparrow} \Delta n_{4\uparrow} \rangle$ in this case vanishes due to the Pauli exclusive principle in the input state $|\Psi_{T_u}\rangle$. It is interesting to note that the correlation $n_{3\uparrow}$ and $n_{4\uparrow}$ of the input entangled triplet state is zero when the beam splitter is ideal, *i.e.*, 50% reflection and 50% transmission. In this case the variance is definitely negative, as shown by the expression in TABLE II (rows 8 and 9, column 3). These negative values indicate that the two electrons with the same spin prefer to locate in different output channels simultaneously in entangled singlet and triplet states. One can see that the correlations $\langle n_{3\uparrow} n_{4\uparrow} \rangle$ are different in all incident states for asymmetric beam splitter (shown by Fig. 7 and Fig. 8). In this case the two correlations and variances of the entangled states behave similarly (shown by solid line and dashed line in Fig. 7, 8, respectively). This again indicates that the output signals $\langle n_{3\uparrow} n_{4\uparrow} \rangle$ and $\langle \Delta n_{3\uparrow} \Delta n_{4\uparrow} \rangle$ are different with respect to Berry phase.

D. The output correlations of different channels with different spins

The rows 10 and 11 in TABLE I and TABLE II give the correlations $\langle n_{3\uparrow} n_{4\downarrow} \rangle$ and $\langle n_{3\downarrow} n_{4\uparrow} \rangle$ for the incoming singlet and triplet states. From those expressions one can see that the four correlations are different in functions of Berry phase, in the transmission, and in the reflection coefficients. This is again possible to devise a coincident

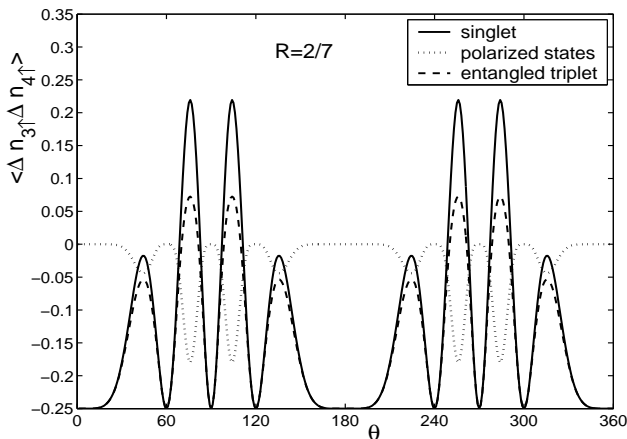


FIG. 8: The variances of the two spin-up electrons in different output channels 3 and 4. The reflection of the beam splitter is $R = 2/7$. The solid line is for the singlet, the dashed line is for the entangled triplet. The dotted line is for both spin-up and spin-down polarized states.

apparatus to distinguish these four states by means of rotating magnetic fields and the external gate voltages. Since the beam splitter is usually constructed by a quantum point contact (QPC)¹⁹. The transmission and reflection are adjusted by the potential barrier, which is controlled by external gate voltages. If the beam splitter is asymmetric, say $R = 2/7$ as shown in Fig. 9 and Fig. 10, the four incident states manifest different behaviors with the polar angle θ . In experiments these coincident signals are easily distinguished. Although the coincidences of polarized states are different, the variances of these states are the same (see Fig. 10). In Fig. 10 the fluctuation correlation is negative for the singlet state and positive for the entangled triplet state showing again the bunching and antibunching property. For a 50:50 beam splitter the singlet and the entangled triplet are irrelevant to transmission and reflection coefficients of the beam splitter. The maximum value of correlation is about 0.3 for the singlet state and 0.5 for the entangled triplet, as shown by Fig.11. The variance $\langle \Delta n_{3\uparrow} \Delta n_{4\downarrow} \rangle$ is almost negative for the singlet state and positive for the entangled triplet, as shown by Fig.12. This shows an electron with spin-up in channel 3 cannot appear simultaneously with an electron with spin-down in channel 4. But it is not true for the entangled triplet. The value of correlation $\langle n_{3\uparrow} n_{4\downarrow} \rangle$ can reach the maximum 1/2, which shows an electron with spin-up in channel 3 appears simultaneously with an electron with spin-down in channel 4 with a probability 1/2. The other case $\langle n_{3\downarrow} n_{4\uparrow} \rangle$ is also 1/2. The sum of these two case is 1. It indicates that these two cases occur definitely and showing the antibunching property. It is not the case for the two polarized states, although their correlations are zero. The reason is that for an individual events $n_{3\uparrow}$ and $n_{4\downarrow}$ are not zero for the two entangled states but $n_{4\downarrow}$ is zero for $|\Psi_{T_u}\rangle$ and $n_{3\uparrow}$ is zero for $|\Psi_{T_d}\rangle$.

One can recover the results in Refs.^{40,41} by removing magnetic fields and sum up the spin indices. The singlet

state $|\Psi_s\rangle$ shows bunching property $\langle n_3 n_4 \rangle = (T - R)^2$ and the triplet state $|\Psi_{T_e}\rangle$ shows antibunching property $\langle n_3 n_4 \rangle = 1$. The average number is 1 for each output channel, i.e., $\langle n_3 \rangle = \langle n_4 \rangle = 1$. It is also consistent with the results of Ref.⁴¹ that the two-particle-occupation probability in one channel is $P(2,0)=2RT$ for Bosons and 0 for Fermions. In our case this corresponds to $\langle n_{3\uparrow} n_{3\downarrow} \rangle = 2RT$ for the singlet state and $\langle n_{3\uparrow} n_{3\downarrow} \rangle = 0$ for the triplet state $|\Psi_{T_u}\rangle$. However, the four states manifest different behavior in magnetic fields. For example, in the case of an ideal beam splitter ($T=R=1/2$) the correlations are $\langle n_{3\uparrow} n_{4\downarrow} \rangle = 0.5 \cos^2 \theta \sin^2 2\gamma_-$ for singlet state $|\Psi_s\rangle$ and $\langle n_{3\uparrow} n_{4\downarrow} \rangle = 0.5 \cos^2 2\gamma_-$ for the triplet state $|\Psi_{T_e}\rangle$, respectively. It is the same for the two polarized states $|\Psi_{T_u}\rangle$ and $|\Psi_{T_d}\rangle$, i.e., $\langle n_{3\uparrow} n_{4\downarrow} \rangle = 0.25 \sin^2 \theta \sin^2 2\gamma_-$. If the beam splitter is not symmetric the correlations $\langle n_{3\uparrow} n_{4\downarrow} \rangle$ are different for these four states, which can be seen from the expressions in TABLE I row 10 or 11.

IV. CONCLUSION

We have investigated the correlations and fluctuations of two-electron states (*i.e.*, singlet and triplet states) affected by two oppositely rotating magnetic fields. We found that the four states pick up Berry phases in different manner manifesting different behaviors in the output correlations and variances. The entangled singlet state shows bunching and antibunching behaviors with respect to Berry phase. The entangled triplet state also shows bunching and antibunching behaviors that differ from that for the singlet state and polarized triplet states. The significant result is that two entangled electrons behave like a composed quasi-particle with total spin zero and unit for the singlet state and the entangled triplet state, respectively. This quasi-particle property is clearly illustrated by Berry phase picked up by the entangled states. Berry phase acquired by the unentangled states shows different behaviors from that of the entangled states. Additionally, the setup discussed in this paper is expected to investigate Berry phase by measuring the correlation and fluctuation using the coincident techniques.

Acknowledgments

This work was supported by the China Natural Science Foundation No. 10274069, 60471052,10225419; the Zhejiang Provincial Natural Foundation M603193; the National Laboratory of Solid State Microstructures: M031802.

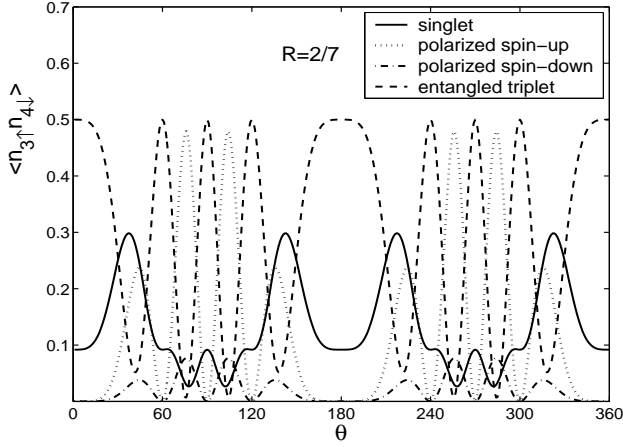


FIG. 9: The correlations of two electrons with opposite spins, i.e., spin-up in channel 3 and spin-down in channel 4. The beam splitter is unsymmetrical with $R = 2/7$. The solid line is for the singlet and the dashed line is for the entangled triplet. The dotted line is for spin-up polarized state and the dot-dashed line is for spin-down polarized state.

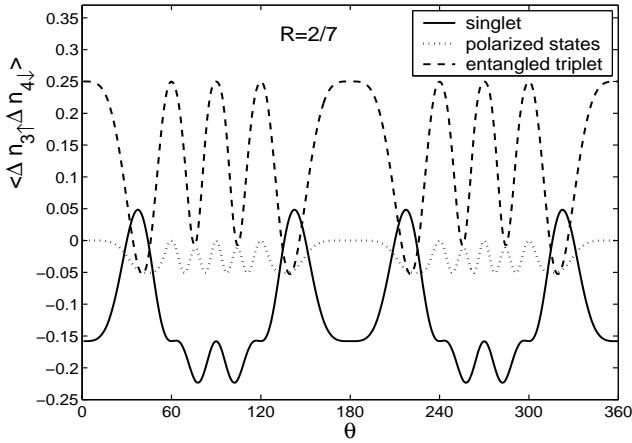


FIG. 10: The variances of the two electrons with spin-up in channel 3 and spin-down in channel 4. The beam splitter is the same as Fig. 9. The solid line is for the singlet and the dashed line is for the entangled triplet. The dotted line is for both polarized states.

TABLE I: The output correlations and average number of electrons for input singlet and triplets ($\Theta = \sin^2 \theta \sin^2 2\gamma_-$)

	$ \Psi_S\rangle$	$ \Psi_{T_e}\rangle$	$ \Psi_{T_u}\rangle$	$ \Psi_{T_d}\rangle$
$\langle n_{3\uparrow} \rangle$	$\frac{1}{2}$	$\frac{1}{2}(1 - 4RT\Theta)$	$1 - R\Theta$	$R\Theta$
$\langle n_{3\downarrow} \rangle$	$\frac{1}{2}$	$\frac{1}{2}(1 - 4RT\Theta)$	$R\Theta$	$1 - R\Theta$
$\langle n_{4\uparrow} \rangle$	$\frac{1}{2}$	$\frac{1}{2}(1 - 4RT\Theta)$	$1 - T\Theta$	$T\Theta$
$\langle n_{4\downarrow} \rangle$	$\frac{1}{2}$	$\frac{1}{2}(1 - 4RT\Theta)$	$T\Theta$	$1 - T\Theta$
$\langle n_{3\uparrow} n_{3\downarrow} \rangle$	$2RT \cos^2 2\gamma_-$	$2RT \cos^2 \theta \sin^2 2\gamma_-$	$RT\Theta$	$RT\Theta$
$\langle n_{4\uparrow} n_{4\downarrow} \rangle$	$2RT \cos^2 2\gamma_-$	$2RT \cos^2 \theta \sin^2 2\gamma_-$	$RT\Theta$	$RT\Theta$
$\langle n_{3\uparrow} n_{4\uparrow} \rangle$	$\frac{1}{2}\Theta$	$\frac{1}{2}(T - R)^2\Theta$	$1 - \Theta$	0
$\langle n_{3\downarrow} n_{4\downarrow} \rangle$	$\frac{1}{2}\Theta$	$\frac{1}{2}(T - R)^2\Theta$	0	$1 - \Theta$
$\langle n_{3\uparrow} n_{4\downarrow} \rangle$	$\frac{1}{2}(T - R)^2 \cos^2 2\gamma_- + \frac{1}{2} \cos^2 \theta \sin^2 2\gamma_-$	$\frac{1}{2} \cos^2 2\gamma_- + \frac{1}{2}(T - R)^2 \cos^2 \theta \sin^2 2\gamma_-$	$T^2\Theta$	$R^2\Theta$
$\langle n_{3\downarrow} n_{4\uparrow} \rangle$	$\frac{1}{2}(T - R)^2 \cos^2 2\gamma_- + \frac{1}{2} \cos^2 \theta \sin^2 2\gamma_-$	$\frac{1}{2} \cos^2 2\gamma_- + \frac{1}{2}(T - R)^2 \cos^2 \theta \sin^2 2\gamma_-$	$R^2\Theta$	$T^2\Theta$

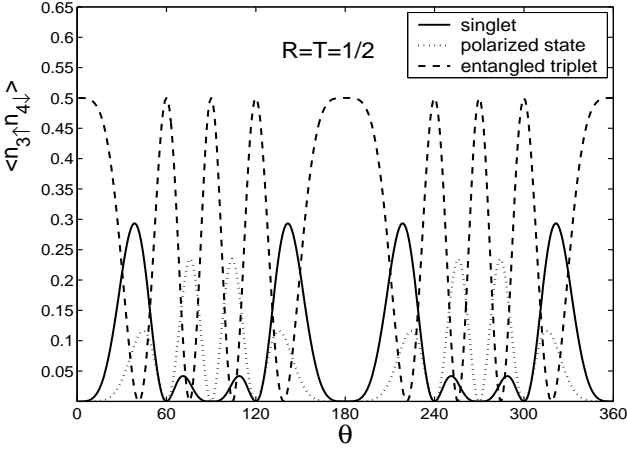


FIG. 11: The correlations of two electrons with opposite spins in different channels 3 and 4. The beam splitter is ideal, i.e. 50:50. The solid line is for the singlet and the dashed line is for the entangled triplet. The dotted line is for both polarized states.

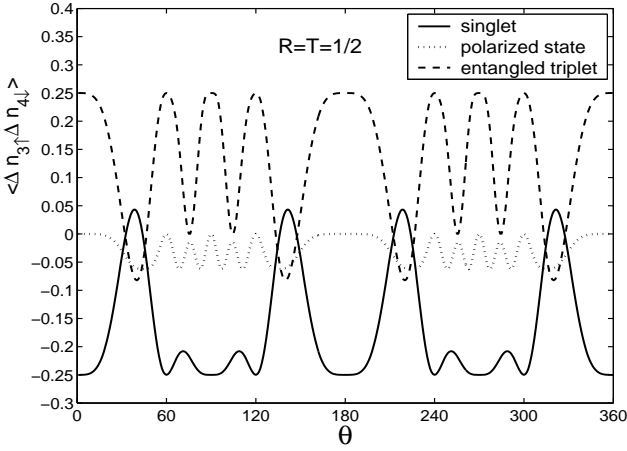


FIG. 12: The variances of the two electrons with spin-up in channel 3 and spin-down in channel 4. The beam splitter is 50:50. The solid line is for the singlet and the dashed line is for the entangled triplet. The dotted line is for both polarized states.

TABLE II: The output variances of electrons for input singlet and triplets ($\Theta = \sin^2 \theta \sin^2 2\gamma_-$)

	$ \Psi_S\rangle$	$ \Psi_{T_e}\rangle$	$ \Psi_{T_u}\rangle$	$ \Psi_{T_d}\rangle$
$\langle \Delta n_{3\uparrow}^2 \rangle$	$\frac{1}{4}$	$\frac{1}{4}(1 - 16R^2T^2\Theta^2)$	$R\Theta(1 - R\Theta)$	$R\Theta(1 - R\Theta)$
$\langle \Delta n_{3\downarrow}^2 \rangle$	$\frac{1}{4}$	$\frac{1}{4}(1 - 16R^2T^2\Theta^2)$	$R\Theta(1 - R\Theta)$	$R\Theta(1 - R\Theta)$
$\langle \Delta n_{4\uparrow}^2 \rangle$	$\frac{1}{4}$	$\frac{1}{4}(1 - 16R^2T^2\Theta^2)$	$T\Theta(1 - T\Theta)$	$T\Theta(1 - T\Theta)$
$\langle \Delta n_{4\downarrow}^2 \rangle$	$\frac{1}{4}$	$\frac{1}{4}(1 - 16R^2T^2\Theta^2)$	$T\Theta(1 - T\Theta)$	$T\Theta(1 - T\Theta)$
$\langle \Delta n_{3\uparrow} \Delta n_{3\downarrow} \rangle$	$2RT \cos^2 2\gamma_- - \frac{1}{4}$	$2RT(\sin^2 2\gamma_- - 2RT\Theta^2) - \frac{1}{4}$	$-R^2\Theta(1 - \Theta)$	$-R^2\Theta(1 - \Theta)$
$\langle \Delta n_{4\uparrow} \Delta n_{4\downarrow} \rangle$	$2RT \cos^2 2\gamma_- - \frac{1}{4}$	$2RT(\sin^2 2\gamma_- - 2RT\Theta^2) - \frac{1}{4}$	$-T^2\Theta(1 - \Theta)$	$-T^2\Theta(1 - \Theta)$
$\langle \Delta n_{3\uparrow} \Delta n_{4\uparrow} \rangle$	$-\frac{1}{4}(1 - 2\Theta)$	$-\frac{1}{4}(1 - 2\Theta) - 4R^2T^2\Theta^2$	$-RT\Theta^2$	$-RT\Theta^2$
$\langle \Delta n_{3\downarrow} \Delta n_{4\downarrow} \rangle$	$-\frac{1}{4}(1 - 2\Theta)$	$-\frac{1}{4}(1 - 2\Theta) - 4R^2T^2\Theta^2$	$-RT\Theta^2$	$-RT\Theta^2$
$\langle \Delta n_{3\uparrow} \Delta n_{4\downarrow} \rangle$	$\frac{1}{4}(1 - 2\Theta) - 2RT \cos^2 2\gamma_-$	$\frac{1}{4}(1 - 2\Theta) + 2RT(2\Theta - \sin^2 2\gamma_- - 2TR\Theta^2)$	$-RT\Theta(1 - \Theta)$	$-RT\Theta(1 - \Theta)$
$\langle \Delta n_{3\downarrow} \Delta n_{4\uparrow} \rangle$	$\frac{1}{4}(1 - 2\Theta) - 2RT \cos^2 2\gamma_-$	$\frac{1}{4}(1 - 2\Theta) + 2RT(2\Theta - \sin^2 2\gamma_- - 2TR\Theta^2)$	$-RT\Theta(1 - \Theta)$	$-RT\Theta(1 - \Theta)$

TABLE III: The input correlations, average number and variances of electrons for singlet and triplets

	$ \Psi_S\rangle$	$ \Psi_{T_e}\rangle$	$ \Psi_{T_u}\rangle$	$ \Psi_{T_d}\rangle$
$\langle n_{1\uparrow} \rangle (\langle \Delta n_{1\uparrow}^2 \rangle)$	$\frac{1}{2}(\frac{1}{4})$	$\frac{1}{2}(\frac{1}{4})$	1(0)	0(0)
$\langle n_{1\downarrow} \rangle (\langle \Delta n_{1\downarrow}^2 \rangle)$	$\frac{1}{2}(\frac{1}{4})$	$\frac{1}{2}(\frac{1}{4})$	0(0)	1(0)
$\langle n_{2\uparrow} \rangle (\langle \Delta n_{2\uparrow}^2 \rangle)$	$\frac{1}{2}(\frac{1}{4})$	$\frac{1}{2}(\frac{1}{4})$	1(0)	0(0)
$\langle n_{2\downarrow} \rangle (\langle \Delta n_{2\downarrow}^2 \rangle)$	$\frac{1}{2}(\frac{1}{4})$	$\frac{1}{2}(\frac{1}{4})$	0(0)	1(0)
$\langle n_{1\uparrow} n_{1\downarrow} \rangle (\langle \Delta n_{1\uparrow} \Delta n_{1\downarrow} \rangle)$	$0(-\frac{1}{4})$	$0(-\frac{1}{4})$	0(0)	0(0)
$\langle n_{2\uparrow} n_{2\downarrow} \rangle (\langle \Delta n_{2\uparrow} \Delta n_{2\downarrow} \rangle)$	$0(-\frac{1}{4})$	$0(-\frac{1}{4})$	0(0)	0(0)
$\langle n_{1\uparrow} n_{2\uparrow} \rangle (\langle \Delta n_{1\uparrow} \Delta n_{2\uparrow} \rangle)$	$0(-\frac{1}{4})$	$0(-\frac{1}{4})$	1(0)	0(0)
$\langle n_{1\downarrow} n_{2\downarrow} \rangle (\langle \Delta n_{1\downarrow} \Delta n_{2\downarrow} \rangle)$	$0(-\frac{1}{4})$	$0(-\frac{1}{4})$	0(0)	1(0)
$\langle n_{1\uparrow} n_{2\downarrow} \rangle (\langle \Delta n_{1\uparrow} \Delta n_{2\downarrow} \rangle)$	$\frac{1}{2}(\frac{1}{4})$	$\frac{1}{2}(\frac{1}{4})$	0(0)	0(0)
$\langle n_{1\downarrow} n_{2\uparrow} \rangle (\langle \Delta n_{1\downarrow} \Delta n_{2\uparrow} \rangle)$	$\frac{1}{2}(\frac{1}{4})$	$\frac{1}{2}(\frac{1}{4})$	0(0)	0(0)

- ¹ A. Einstein, B. Podolsky and N. Rosen, Phys. Rev. **47**, 777(1935).
- ² E. Schrödinger, Naturwissenschaften, **23**, 807(1935); **23**, 844(1935).
- ³ J. S. Bell, Physics **1**, 195(1964); Rev. Mod. Phys. **38**, 447(1966); *Speakable and Unsayable in Quantum Mechanics* (Cambridge University Press, Cambridge, 1987).
- ⁴ A. Zeilinger, Rev. Mod. Phys. **71**, S288(1999). M. Aspelmeyer, *et al*, Science **301** 621-623(2003); CZ Peng, *et al*, Phys. Rev. Lett. **94** 150501(2005); DL Moehring, *et al* Phys. Rev. Lett. **93** 090410(2004).
- ⁵ NF Bell, AA Rawlinson, RF Sawyer, Physics Letters B **573** (1-4): 86-93 (2003); R. A. Bertlmann *et al* Phys. Rev. A **63** 062112(2001).
- ⁶ C. H. Bennett, Phys. Today **48** 24(1995); S. Lloyd, Science **261** 1569(1993).
- ⁷ P. Samuelsson, E. V. Sukhorukov, and M. Büttiker, Phys. Rev. B **70** 115330(2004).
- ⁸ P. Samuelsson, E. V. Sukhorukov, and M. Büttiker Phys. Rev. Lett. **91** 157002(2003).
- ⁹ P. Samuelsson, E. V. Sukhorukov, and M. Büttiker Phys. Rev. Lett. **92** 026805(2004).
- ¹⁰ Daniel Loss and David P. diVincenzo Phys. Rev. B **57** 120(1998).
- ¹¹ Guido Burkard and Daniel Loss Phys. Rev. Lett. **91** 087903(2003).
- ¹² Daniel S. Saraga and Daniel Loss Phys. Rev. Lett. **90** 166803(2003).
- ¹³ Guido Burkard, Daniel Loss, and Eugene V. Sukhorukov Phys. Rev. B **61** R16303(2000).
- ¹⁴ Nikolai M. Chtchelkatchev, Gianni Blatter, Gordey B. Lesovik, and Thierry Martin Phys. Rev. B. **66** 161320(2002).
- ¹⁵ A. V. Lebedev, G. Blatter, C. W. J. Beenakker, and G. B. Lesovik Phys. Rev. B. **69** 235312(2004).
- ¹⁶ J. M. Kikkawa and D. D. Awschalom, Nature **397**, 139(1999); Phys. Rev. Lett. **80**, 4313(1998).
- ¹⁷ P. Recher, E. V. Sukhorukov, and D. Loss, Phys. Rev. B **63**, 165314(2001). P. Recher and D. Loss, Phys. Rev. B, **65**, 165327(2002).
- ¹⁸ G. B. Lesovik, T. Martin, and G. Blatter, Eur. Phys. J. B **24**,287(2001). C. Bena, S. Vishveshwara, L. Balents, and M. P. A. Fisher, Phys. Rev. Lett. **89**, 037901(2002).
- ¹⁹ R. C. Liu, B. Odom, Y. Yamamoto, and S. Tarucha, Nature **391**, 263(1998).
- ²⁰ J. Carlos Egues, Guido Burkard, and Daniel Loss, Phys. Rev. Lett. **89**, 176401(2002).
- ²¹ HQ Zhou, U. Lundin, S. Y. Cho, and R. H. Mckenzie, Phys. Rev. B **69**, 113308(2004).
- ²² M. V. Berry, Proc. R. Soc. London Ser. A **392**, 45(1984)
- ²³ Marie Ericsson, Arun K. Pati, Erik Sjöqvist, Johan Brännlund, and Daniel K. L. Oi Phys. Rev. Lett. **91**, 090405(2003).
- ²⁴ R. G. Unanyan and M. Fleischhauer, Phys. Rev. A **69**, 050302(2004).
- ²⁵ Jonathan A. Jones, Vlatko Vedral, Artur Ekert, and Gluseppe Castagnoll, Nature **403**, 869(2000).
- ²⁶ Artur Ekert, Marie Ericsson, Patrick Hayden, Hitoshi Inamori, Jonathan A. Jones Daniel K. L. Oi, and Vlatko Vedral, quant-ph/0004015.
- ²⁷ Shi-Liang Zhu and Z. D. Wang, Phys. Rev. A **67**, 022319(2003).
- ²⁸ N. A. Gershenfeld and I. L. Chung, Science **275**, 350(1997).
- ²⁹ J. Samuel and R. Bhandari, Phys. Rev. Lett. **60**, 2339(1988).
- ³⁰ T. Bitter and D. Dubbers, Phys. Rev. Lett. **59**, 2156(1987).
- ³¹ Y. Hasegawa, R. Loidl, G. Badurek, M. Baron, N. Manini, F. Pistolesi, and H. Rauch, Phys. Rev. A **65**, 052111(2002).
- ³² Y. Taguchi, Y. Oohara, H. Yoshizawa, N. Nagaosa, Y. Tokura, Science **291**, 2573(2001).
- ³³ Daniel Loss, Paul Goldbart, and A. V. Balatsky, Phys. Rev. Lett. **65**, 1655(1990).
- ³⁴ Erik Sjöqvist, Phys. Rev. A, **62**, 022109(2000).
- ³⁵ D M Tong, L C Kwek and C H Oh, J. Phys. A: Math. Gen. **36**, 1149(2003).
- ³⁶ D. M. Tong, E. Sjöqvist, L. D. Kwek, C. H. Oh, and M. Ericsson, Phys. Rev. A **68**, 022106(2003).
- ³⁷ F. Mezei, *Neutron Spin Echo*, Lecture Notes in Physics, Springer(1980).
- ³⁸ X. B. Wang and M. Keiji, Phys. Rev. Lett. **87**, 097901(2001); **88**, 179901(2002). X. B. Wang and M. Keiji, Phys. Rev. Lett. **87**, 097901(2001); **88**, 179901(2002).
- ³⁹ R. Gähler, *et al*, Physica B **180**, 899(1992).
- ⁴⁰ Rodney Loudon, Phys. Rev. B **58**, 4904(1998).
- ⁴¹ Ya. M. Blanter, M. Büttiker, Physics Report **336**, 1-166(2000).